

MIT Open Access Articles

Standard Thermodynamic Functions of Tripeptides N-Formyl-L-Methionyl-L-Leucyl-L-Phenylalaninol and N-Formyl-L-Methionyl-L-Leucyl-L-Phenylalanine Methyl Ester

The MIT Faculty has made this article openly available. **Please share** how this access benefits you. Your story matters.

Citation: Markin, Alexey V., Evgeny Markhasin, Semen S. Sologubov, Natalia N. Smirnova, and Robert G. Griffin. "Standard Thermodynamic Functions of Tripeptides N-Formyl-L-Methionyl-L-Leucyl-L-Phenylalaninol and N-Formyl-L-Methionyl-L-Leucyl-L-Phenylalanine Methyl Ester." *Journal of Chemical & Engineering Data* 59, no. 4 (April 10, 2014): 1240–1246. © 2014 American Chemical Society

As Published: <http://dx.doi.org/10.1021/je400879v>

Publisher: American Chemical Society (ACS)

Persistent URL: <http://hdl.handle.net/1721.1/96212>

Version: Final published version: final published article, as it appeared in a journal, conference proceedings, or other formally published context

Terms of Use: Article is made available in accordance with the publisher's policy and may be subject to US copyright law. Please refer to the publisher's site for terms of use.



Standard Thermodynamic Functions of Tripeptides *N*-Formyl-L-methionyl-L-leucyl-L-phenylalaninol and *N*-Formyl-L-methionyl-L-leucyl-L-phenylalanine Methyl Ester

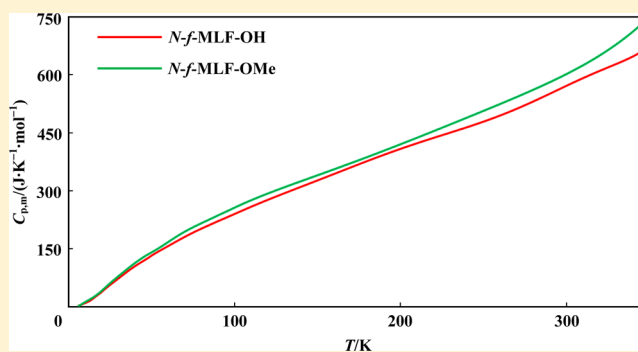
Alexey V. Markin,^{*,†} Evgeny Markhasin,[‡] Semen S. Sologubov,[†] Natalia N. Smirnova,[†] and Robert G. Griffin[‡]

[†]Lobachevsky State University of Nizhni Novgorod, 23/5 Gagarin Avenue, 603950, Nizhni Novgorod, Russia

[‡]Massachusetts Institute of Technology, 150 Albany Street, Cambridge, Massachusetts 02139, United States

ABSTRACT: The heat capacities of tripeptides *N*-formyl-L-methionyl-L-leucyl-L-phenylalaninol (*N*-f-MLF-OH) and *N*-formyl-L-methionyl-L-leucyl-L-phenylalanine methyl ester (*N*-f-MLF-OMe) were measured by precision adiabatic vacuum calorimetry over the temperature range from $T = (6 \text{ to } 350) \text{ K}$. The tripeptides were stable over this temperature range, and no phase change, transformation, association, or thermal decomposition was observed. The standard thermodynamic functions: molar heat capacity $C_{p,m}$, enthalpy $H(T) - H(0)$, entropy $S(T)$, and Gibbs energy $G(T) - H(0)$ of peptides were calculated over the range from $T = (0 \text{ to } 350) \text{ K}$. The low-temperature ($T \leq 50 \text{ K}$) heat capacities dependencies were analyzed using the Debye's and the multifractal theories.

The standard entropies of formation of peptides at $T = 298.15 \text{ K}$ were calculated.



INTRODUCTION

The investigation of physicochemical properties of amino acids and peptides attracts much attention, since these systems can be used as molecular materials, drugs, and biomimetics.¹

Furthermore, certain peptides are used as model systems to design and test experiments for protein studies.^{2,3} For example, tripeptides *N*-formyl-L-methionyl-L-leucyl-L-phenylalaninol (*N*-f-MLF-OH) and *N*-formyl-L-methionyl-L-leucyl-L-phenylalanine methyl ester (*N*-f-MLF-OMe) have been used in solid state NMR spectroscopy for developing and testing NMR experiments.^{4–6} These tripeptides have also been used as models for structural studies.⁷

There are no data on heat capacities and thermodynamic properties of these tripeptides found in the literature. Those are, however, necessary as the fundamental data for peptides and proteins and to calculate thermophysical properties for the model system. Therefore, the purpose of the present study was to measure heat capacities of tripeptides *N*-f-MLF-OH and *N*-f-MLF-OMe over the temperature range from $T = (6 \text{ to } 350) \text{ K}$, to calculate the standard ($p = 0.1 \text{ MPa}$) thermodynamic functions $C_{p,m}$, $H(T) - H(0)$, $S(T)$, and $G(T) - H(0)$, to determine the characteristic temperatures and fractal dimensions D , and to calculate the standard entropies of formation of *N*-f-MLF-OH (cr) and *N*-f-MLF-OMe (cr) at $T = 298.15 \text{ K}$.

EXPERIMENTAL SECTION

Synthesis and Characterization of Tripeptides. Tripeptides *N*-formyl-L-Met-L-Leu-L-Phe-OH (lot 2500845) and *N*-

formyl-L-Met-L-Leu-L-Phe-OMe (lot 1016424) were obtained from Bachem (King of Prussia, PA). Solid state NMR structure and X-ray structure of *N*-f-MLF-OH and *N*-f-MLF-OMe were described previously.^{7,8} Structural models of the studied samples are presented in Figure 1. The molecular formulas $C_{21}H_{31}N_3O_5S$ for *N*-f-MLF-OH and $C_{22}H_{33}N_3O_5S$ for *N*-f-MLF-OMe were confirmed by elemental analysis. In accordance with elemental analysis, high-performance liquid chromatography (HPLC), and thin layer chromatography (TLC) data, the content of the main compounds in the studied samples was at least 0.99 molar fraction. The information for the studied tripeptides is listed in Table 1.

Adiabatic Calorimetry. A precision automatic adiabatic calorimeter (Block Calorimetric Thermophysical, BCT-3) was used to measure heat capacities over the temperature range from $T = (6 \text{ to } 350) \text{ K}$. The design and operation of an adiabatic calorimeter are described in detail elsewhere.^{9,10} A calorimetric cell is a thin-walled cylindrical vessel made from titanium with a volume of $1.5 \cdot 10^{-6} \text{ m}^3$. Its mass is $(1.626 \pm 0.005) \text{ g}$. A miniature iron–rhodium resistance thermometer (nominal resistance 100Ω , was calibrated on ITS-90 standard by the Russian Metrology Research Institute, Moscow region, Russia) was used to measure the temperature of the sample. The temperature difference between the ampule and an

Received: October 3, 2013

Accepted: February 26, 2014

Published: March 13, 2014

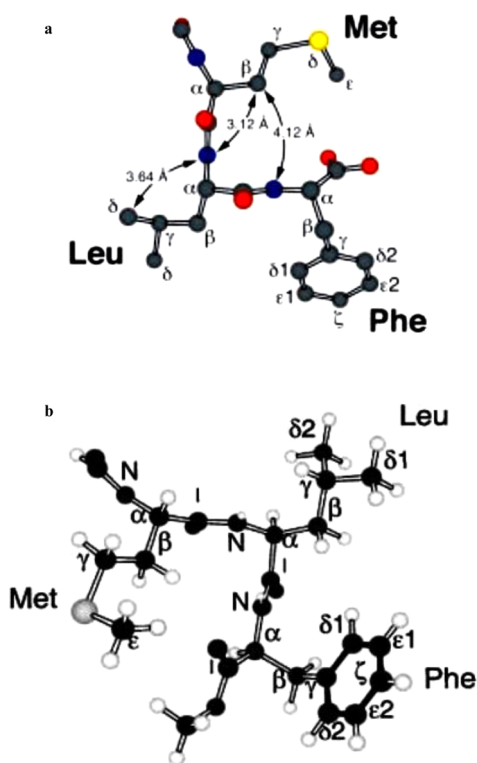


Figure 1. Structural models of the tripeptides under study. (a) *N*-formyl-L-Met-L-Leu-L-Phe-OH⁷; (b) *N*-formyl-L-Met-L-Leu-L-Phe-OMe⁸.

adiabatic shield was controlled by a four-junction copper–iron–chromel thermocouple. The sensitivity of the thermometric circuit was $1 \cdot 10^{-3}$ K, and that of the analog-to-digital converter was $0.1 \mu\text{V}$. The accuracy of the calorimeter was verified using standard reference samples (K-2 benzoic acid and $\alpha\text{-Al}_2\text{O}_3$)^{11,12} prepared by the Institute of Metrology of the State Standard Committee of the Russian Federation. The deviations of our results from the recommended values of NIST¹¹ are within $0.02 C_{p,m}$ between $T = (6 \text{ to } 20) \text{ K}$, $0.005 C_{p,m}$ between $T = (20 \text{ to } 40) \text{ K}$, and $0.002 C_{p,m}$ in the temperature range from $T = (40 \text{ to } 350) \text{ K}$. The standard uncertainty for the temperature was $u(T) = 0.01 \text{ K}$, and the relative standard uncertainty for the enthalpies of fusion was $u_r(\Delta_{\text{fus}}H) = 0.002$.

Heat Capacities Measurements. Samples of 0.2438 g of *N*-f-MLF-OH ($M = 437.56 \text{ g}\cdot\text{mol}^{-1}$) and 0.2716 g of *N*-f-MLF-OMe ($M = 451.59 \text{ g}\cdot\text{mol}^{-1}$) were placed in a calorimetric ampule, and it was then filled with dry helium gas (4 kPa, room temperature) to facilitate the heat exchanging process. Initially, the samples were cooled to the temperature of the measurement onset ($\sim 6 \text{ K}$) at a rate of $0.01 \text{ K}\cdot\text{s}^{-1}$. Then the samples were heated in $(0.5 \text{ to } 2) \text{ K}$ increments at a rate of $0.01 \text{ K}\cdot\text{s}^{-1}$. The sample temperature was recorded after an equilibration period (temperature drift $< 0.01 \text{ K}\cdot\text{s}^{-1}$, approximately 10 min per experimental point).

Table 1. Sample Information

chemical name	source	state	mole fraction purity	purification method	analysis method
<i>N</i> -f-MLF-OH ^a	Bachem (King of Prussia, PA)	powder	0.99	HPLC ^c , TLC ^d	TLC
<i>N</i> -f-MLF-OMe ^b	Bachem (King of Prussia, PA)	powder	0.99	HPLC, TLC	TLC

^a*N*-f-MLF-OH = *N*-formyl-L-Met-L-Leu-L-Phe-OH. ^b*N*-f-MLF-OMe = *N*-formyl-L-Met-L-Leu-L-Phe-OMe. ^cHigh-performance liquid chromatography. ^dThin layer chromatography.

The experimental values of $C_{p,m}$ (157 and 185 points for *N*-f-MLF-OH and *N*-f-MLF-OMe, respectively) were collected using liquid helium as a cryogen in the intervals from $T = (6 \text{ to } 88) \text{ K}/(6 \text{ to } 91) \text{ K}$ (Series 1) and using liquid nitrogen in the intervals from $T = (84 \text{ to } 349) \text{ K}/(91 \text{ to } 343) \text{ K}$ (Series 2) for *N*-f-MLF-OH and *N*-f-MLF-OMe, respectively.

Heat capacities of the samples were between (55 to 83) % of the overall heat capacity of the calorimetric ampule. The molar masses were calculated from the IUPAC table of atomic weights.¹³

RESULTS AND DISCUSSION

Heat Capacities. Experimental data for the molar heat capacities of *N*-f-MLF-OH and *N*-f-MLF-OMe over the temperature range from $T = (6 \text{ to } 350) \text{ K}$ are given in Tables 2 and 3 and presented in Figure 2. Heat capacities of the samples rise gradually with temperature increasing. The tripeptides were stable over the studied temperature range, and no phase change, transformation, association, or thermal decomposition was observed.

The experimental data were smoothed using least-squares polynomial fits as follows:

$$C_{p,m} = \begin{cases} \sum_{i=0}^7 A_i \ln\left(\frac{T}{30}\right)^i, & 6 \text{ K} \leq T \leq 40 \text{ K} \\ \sum_{i=0}^6 B_i \ln\left(\frac{T}{30}\right)^i, & 40 \text{ K} \leq T \leq 350 \text{ K} \end{cases}$$

where A_i and B_i are polynomial coefficients. Relative standard uncertainty for the heat capacities $u_r(C_{p,m}) = 0.006$ in the temperature range from $T = (6 \text{ to } 40) \text{ K}$ and $u_r(C_{p,m}) = 0.003$ between $T = (40 \text{ to } 350) \text{ K}$. The relative deviations of experimental data from the smoothing functions were listed in Figure 3.

The temperature dependencies of heat capacities of the two tripeptides are similar below 50 K. This tendency can be expected, since skeletal vibrations provide the main contribution to heat capacities in this range.

Low-temperature heat capacities data were also analyzed using the Debye theory¹⁴ and the multifractal theory of heat capacity.¹⁵

According to the fractal theory,¹⁵

$$C(T, D) = 3D(D + 1)Nkr \left[\frac{T}{\Theta} \right]^D \cdot \int_0^{\Theta/T} \frac{x^D}{\exp(x) - 1} dx - 3DNkr \cdot \frac{\Theta/T}{\exp(\Theta/T) - 1} \quad (1)$$

Equation 1 can be written as eq 2:

$$C_v = 3D(D + 1)kN\gamma(D + 1)\xi(D + 1)(T/\Theta_{\text{max}})^D \quad (2)$$

Table 2. Experimental Molar Heat Capacities of Crystalline N-f-MLF-OH ($M = 437.56 \text{ g}\cdot\text{mol}^{-1}$)^a

T/K	$C_{p,m}/\text{J}\cdot\text{K}^{-1}\cdot\text{mol}^{-1}$	T/K	$C_{p,m}/\text{J}\cdot\text{K}^{-1}\cdot\text{mol}^{-1}$	T/K	$C_{p,m}/\text{J}\cdot\text{K}^{-1}\cdot\text{mol}^{-1}$
Series 1					
6.07	3.03	11.08	11.8	32.83	82.65
6.20	3.36	11.52	12.5	35.21	90.33
6.39	3.61	11.95	13.4	37.62	97.96
6.58	3.95	12.39	14.6	40.05	105.2
6.77	4.19	12.85	15.8	42.50	112.5
6.95	4.46	13.31	17.0	44.97	118.8
7.13	4.64	13.78	18.1	47.45	124.6
7.31	5.02	14.29	19.5	49.34	130.5
7.66	5.64	14.76	21.3	50.80	134.7
7.84	5.84	15.24	23.4	54.20	143.5
8.02	6.22	15.73	24.77	56.90	149.6
8.19	6.56	16.23	26.48	59.00	154.9
8.37	6.65	16.73	28.13	61.10	159.7
8.55	7.15	17.24	29.68	64.20	167.0
8.72	7.42	17.76	31.41	67.25	174.4
8.92	7.88	18.29	32.48	69.89	180.6
9.10	8.16	18.81	34.25	72.43	186.4
9.27	8.57	19.34	36.24	75.35	193.1
9.44	8.94	19.87	38.47	77.93	197.9
9.62	9.38	21.37	44.16	80.00	202.2
9.80	9.59	23.57	51.73	83.20	207.8
9.98	10.0	25.84	59.41	85.77	213.1
10.26	10.5	28.14	67.29	87.50	216.0
10.67	11.0	30.47	75.15		
Series 2					
83.90	210.0	179.11	375.4	267.60	507.4
86.84	215.7	181.51	379.4	270.95	513.7
90.20	221.9	182.44	381.6	273.80	518.1
93.70	228.4	185.90	386.5	277.59	524.9
96.85	234.0	188.64	391.0	280.88	532.5
100.96	241.6	192.20	397.2	282.23	537.3
104.77	248.7	195.77	402.6	285.29	542.7
110.00	259.0	199.33	408.1	288.58	549.3
114.57	267.0	200.73	410.2	293.30	557.4
118.10	273.3	204.09	414.5	297.80	565.3
121.64	279.0	207.65	420.2	301.54	573.1
125.17	285.5	211.20	423.3	304.73	582.3
128.71	291.7	214.75	429.4	307.89	588.5
132.24	297.1	218.30	433.6	311.05	593.5
135.78	303.1	220.18	436.8	313.20	599.5
139.31	309.8	223.47	441.4	316.00	602.2
142.85	315.6	226.98	445.4	318.33	605.8
146.39	321.0	230.48	451.2	321.40	610.8
149.76	327.1	234.30	456.4	323.50	615.2
153.11	331.8	238.80	462.3	326.18	619.5
156.66	336.9	242.45	469.1	329.70	626.6
158.99	341.8	244.90	472.6	331.99	630.9
162.34	347.3	246.30	474.8	334.86	638.4
165.75	352.2	247.70	474.8	337.66	643.6
169.10	358.5	250.00	478.6	340.47	648.2
171.03	363.2	253.99	484.7	342.70	653.7
174.39	366.7	257.43	489.4	346.02	662.6
176.01	369.0	260.84	494.6	348.70	668.4
177.95	374.1	264.24	501.0		

^aStandard uncertainty for temperature $u(T) = 0.01 \text{ K}$ and relative standard uncertainty for the heat capacities $u_r(C_{p,m}) = 0.02$ in the temperature range from $T = (6 \text{ to } 15) \text{ K}$, $u_r(C_{p,m}) = 0.005$ between $T = (15 \text{ to } 40) \text{ K}$, and $u_r(C_{p,m}) = 0.002$ in the temperature range from $T = (40 \text{ to } 349) \text{ K}$.

where D is the fractal dimension, N is the number of atoms in a molecular unit, k is the Boltzmann constant, $\gamma(D + 1)$ is the γ -

function, $\xi(D + 1)$ is the Riemann ξ -function, and Θ_{\max} is the characteristic temperature. For a particular solid $3D(D + 1)$

Table 3. Experimental Molar Heat Capacities of Crystalline *N*-f-MLF-OMe ($M = 451.59 \text{ g}\cdot\text{mol}^{-1}$)^a

T/K	$C_{p,m}/\text{J}\cdot\text{K}^{-1}\cdot\text{mol}^{-1}$	T/K	$C_{p,m}/\text{J}\cdot\text{K}^{-1}\cdot\text{mol}^{-1}$	T/K	$C_{p,m}/\text{J}\cdot\text{K}^{-1}\cdot\text{mol}^{-1}$
Series 1					
6.02	2.60	10.27	13.2	32.65	88.71
6.13	2.71	10.63	14.1	35.04	96.64
6.28	2.91	11.04	15.0	37.44	105.0
6.43	3.21	11.45	16.0	39.87	112.9
6.59	3.52	11.88	17.1	42.32	120.6
6.73	3.88	12.29	18.0	44.78	127.7
6.88	4.29	12.79	19.2	47.26	134.1
7.04	4.56	13.24	20.4	49.75	139.9
7.19	4.97	13.71	21.7	52.01	145.9
7.35	5.42	14.18	22.7	54.78	153.1
7.52	5.83	14.65	24.1	57.30	160.1
7.66	6.28	15.12	25.3	59.87	167.1
7.84	6.73	15.60	26.78	62.41	174.3
7.98	7.23	15.99	28.00	64.96	181.3
8.17	7.72	16.64	29.85	66.90	186.5
8.33	8.13	17.10	31.58	70.06	194.1
8.50	8.58	17.62	33.24	72.60	201.0
8.70	9.08	18.10	34.79	75.15	206.0
8.84	9.48	18.78	37.21	77.73	212.1
8.98	9.89	19.22	38.75	80.10	216.1
9.13	10.3	19.72	40.59	82.93	221.7
9.30	10.7	21.41	47.32	85.50	227.0
9.45	11.0	23.40	55.20	88.20	232.3
9.62	11.5	25.67	63.45	90.85	237.1
9.78	11.8	27.96	71.89		
9.95	12.3	30.29	80.50		
Series 2					
90.60	238.4	176.09	381.5	254.83	514.5
93.51	243.4	179.50	385.9	257.07	518.7
96.19	248.8	182.11	390.6	259.30	523.3
98.88	253.3	184.71	394.8	261.50	528.0
101.58	258.9	187.31	398.3	263.68	532.6
104.28	264.0	189.90	402.2	265.84	535.2
106.98	269.4	192.49	407.4	267.99	539.2
109.69	274.9	195.07	411.8	270.16	543.2
112.38	279.5	197.64	416.1	272.34	547.3
115.08	284.3	200.20	420.0	274.50	552.1
117.78	289.3	202.74	423.8	276.67	554.9
120.47	293.3	205.27	428.2	277.10	557.8
123.16	297.5	207.77	433.6	279.97	561.2
125.85	302.5	210.28	436.5	282.11	564.9
128.53	306.7	212.77	442.5	284.23	568.8
131.22	310.6	215.23	446.4	286.34	571.5
133.99	316.2	217.60	450.8	288.80	578.0
136.67	319.1	220.02	455.6	290.49	581.0
139.35	323.5	222.40	459.1	292.53	584.6
142.02	328.1	224.71	463.1	294.54	587.8
144.68	332.5	227.02	467.1	296.39	591.6
147.35	336.5	229.33	471.1	298.40	596.2
150.01	340.6	231.66	475.2	300.24	601.4
152.68	344.7	234.00	478.4	302.09	606.6
155.33	348.5	236.36	484.2	304.77	614.7
157.99	352.9	238.72	488.0	307.42	619.1
160.64	357.2	241.09	490.9	309.83	624.8
163.28	361.6	243.46	493.2	312.19	631.0
165.92	365.7	245.83	498.9	314.41	635.0
168.56	368.7	248.18	503.0	316.68	638.7
171.19	373.7	250.50	507.1	318.91	645.4
174.60	377.8	252.78	509.6	321.09	652.2
323.22	661.1	332.75	688.8	340.17	710.6

Table 3. continued

T/K	$C_{p,m}/\text{J}\cdot\text{K}^{-1}\cdot\text{mol}^{-1}$	T/K	$C_{p,m}/\text{J}\cdot\text{K}^{-1}\cdot\text{mol}^{-1}$	T/K	$C_{p,m}/\text{J}\cdot\text{K}^{-1}\cdot\text{mol}^{-1}$
Series 2					
325.19	665.5	334.50	691.9	341.74	717.0
327.12	669.6	335.18	695.0	343.27	723.9
329.13	677.2	336.88	700.5		
330.96	681.9	338.54	704.4		

^aStandard uncertainty for temperature $u(T) = 0.01$ K and relative standard uncertainty for the heat capacities $u_r(C_{p,m}) = 0.02$ in the temperature range from $T = (6$ to $15)$ K, $u_r(C_{p,m}) = 0.005$ between $T = (15$ to $40)$ K, and $u_r(C_{p,m}) = 0.002$ in the temperature range from $T = (40$ to $343)$ K.

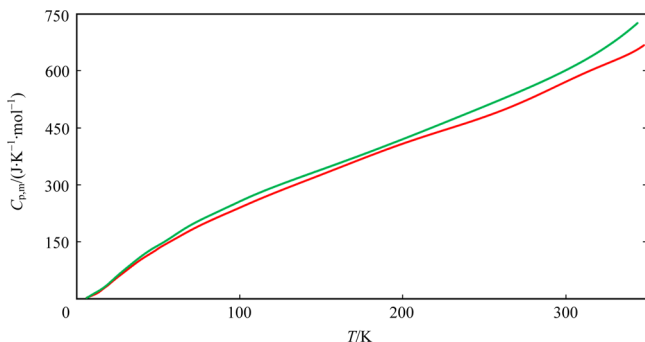


Figure 2. Experimental molar heat capacities $C_{p,m}$ of the tripeptides under study. Red line, *N*-formyl-L-Met-L-Leu-L-Phe-OH; green line, *N*-formyl-L-Met-L-Leu-L-Phe-OMe.

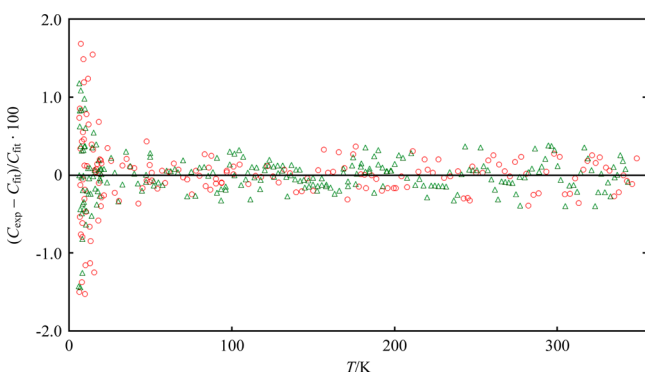


Figure 3. Plot of deviations of experimental data from fitted. Red \circ , *N*-formyl-L-Met-L-Leu-L-Phe-OH; green \triangle , *N*-formyl-L-Met-L-Leu-L-Phe-OMe.

$kN\gamma(D+1)\xi(D+1)(1/\Theta_{\max})^D = A$ is a constant value, and eq 2 can be rewritten as follows:

$$\ln C_v = \ln A + D \ln T \quad (3)$$

which can be used to obtain D and Θ_{\max} .

Since below $T = 50$ K the experimental values of $C_{p,m}$ are equal to C_v . Thus, experimental data in the range from $T = (20$ to $50)$ K were used and yielded $D = 1.6$, $\Theta_{\max} = 202.8$ K for *N*-f-MLF-OH, and $D = 1.8$, $\Theta_{\max} = 183.0$ K for *N*-f-MLF-OMe. The relative standard uncertainty for the characteristic temperatures is $u_r(\Theta_{\max}) = 0.007$.

According to the multifractal model of the theory of heat capacity of solids,¹⁵ $D = 1$ corresponds to solids with a chain structure, $D = 2$ corresponds to ones with a layered structure, and $D = 3$ corresponds to ones with a spatial structure, characterized by comparable interactions in all three dimensions. The obtained values of D point to the chain-layered structure for both tripeptides.

The Debye theory was used to fit the experimental data in the range from $T = (6$ to $12)$ K and extrapolate it to 0 K.¹⁴

Table 4. Smoothed Molar Heat Capacities and Thermodynamic Functions of Crystalline *N*-f-MLF-OH ($M = 437.56$ g·mol⁻¹) at Pressure $p = 0.1$ MPa^a

T/K	$C_{p,m}$ J·K ⁻¹ ·mol ⁻¹	$[H(T) - H(0)]$ kJ·mol ⁻¹	$S(T)$ J·K ⁻¹ ·mol ⁻¹	$-[G(T) - H(0)]$ kJ·mol ⁻¹
5	1.75	0.00218	0.588	0.000736
10	9.91	0.0297	4.07	0.0110
15	22.2	0.106	10.1	0.0452
20	38.84	0.2581	18.73	0.1165
25	56.77	0.4981	29.36	0.2358
30	73.31	0.8234	41.17	0.4118
40	105.1	1.720	66.75	0.9502
50	132.6	2.907	93.13	1.749
60	157.1	4.358	119.5	2.813
70	180.9	6.049	145.5	4.139
80	202.1	7.966	171.1	5.722
90	221.4	10.08	196.0	7.558
100	240.1	12.39	220.3	9.641
110	258.7	14.89	244.1	11.96
120	276.5	17.56	267.4	14.52
130	293.6	20.41	290.1	17.31
140	310.2	23.43	312.5	20.32
150	326.8	26.62	334.5	23.56
160	343.6	29.97	356.1	27.01
170	360.3	33.49	377.5	30.68
180	376.9	37.18	398.5	34.56
190	393.0	41.03	419.4	38.65
200	408.4	45.03	439.9	42.95
210	422.9	49.19	460.2	47.45
220	436.8	53.49	480.2	52.15
230	450.3	57.93	499.9	57.05
240	464.2	62.50	519.4	62.15
250	478.7	67.21	538.6	67.44
260	494.5	72.08	557.7	72.92
270	511.9	77.11	576.7	78.59
280	530.8	82.32	595.6	84.45
290	550.9	87.73	614.6	90.50
298.15	567.6	92.29	630.1	95.57
300	571.3	93.34	633.6	96.74
310	591.2	99.16	652.7	103.2
320	609.9	105.2	671.7	109.8
330	627.7	111.4	690.8	116.6
340	647.1	117.7	709.8	123.6
348	667.6	123.0	725.1	129.4

^aStandard uncertainty for temperature $u(T) = 0.01$ K and relative standard uncertainty for the heat capacities $u_r(C_{p,m}) = 0.02$ in the temperature range from $T = (6$ to $15)$ K, $u_r(C_{p,m}) = 0.005$ between $T = (15$ to $40)$ K, and $u_r(C_{p,m}) = 0.002$ in the temperature range from $T = (40$ to $348)$ K.

$$C_{p,m} = nD(\Theta_D/T) \quad (4)$$

Table 5. Smoothed Molar Heat Capacities and Thermodynamic Functions of Crystalline *N*-f-MLF-OMe ($M = 451.59 \text{ g}\cdot\text{mol}^{-1}$) at Pressure $p = 0.1 \text{ MPa}^a$

T/K	$C_{p,m}$	$[H(T) - H(0)]$	$S(T)$	$-[G(T) - H(0)]$
	$\text{J}\cdot\text{K}^{-1}\cdot\text{mol}^{-1}$	$\text{kJ}\cdot\text{mol}^{-1}$	$\text{J}\cdot\text{K}^{-1}\cdot\text{mol}^{-1}$	$\text{kJ}\cdot\text{mol}^{-1}$
5	1.99	0.00249	0.664	0.000831
10	12.5	0.0342	4.63	0.0121
15	25.1	0.127	12.0	0.0528
20	41.76	0.2921	21.37	0.1354
25	61.13	0.5495	32.77	0.2697
30	79.28	0.9009	45.54	0.4652
40	113.3	1.867	73.10	1.057
50	140.8	3.145	101.5	1.931
60	167.6	4.683	129.5	3.086
70	194.3	6.496	157.4	4.520
80	216.1	8.552	184.8	6.231
90	236.3	10.81	211.4	8.213
100	256.4	13.28	237.4	10.46
110	275.6	15.94	262.7	12.96
120	292.9	18.78	287.4	15.71
130	309.1	21.79	311.5	18.70
140	324.7	24.96	335.0	21.94
150	340.1	28.29	357.9	25.40
160	355.6	31.77	380.4	29.09
170	371.3	35.40	402.4	33.01
180	387.3	39.19	424.1	37.14
190	403.7	43.15	445.5	41.49
200	420.3	47.27	466.6	46.05
210	437.2	51.55	487.5	50.82
220	454.3	56.03	508.2	55.80
230	471.6	60.64	528.8	60.98
240	489.0	65.44	549.2	66.38
250	506.5	70.42	569.6	71.97
260	524.3	75.58	589.8	77.77
270	542.4	80.91	609.9	83.76
280	561.1	86.43	630.0	89.96
290	580.7	92.13	650.0	96.36
298.15	597.6	96.94	666.3	101.7
300	601.6	98.05	670.0	103.0
310	624.4	104.2	690.1	109.8
320	649.7	110.5	710.3	116.8
330	678.4	117.2	730.8	124.0
340	711.3	124.1	751.5	131.4
344	726.0	127.0	759.9	134.4

^aStandard uncertainty for temperature $u(T) = 0.01 \text{ K}$ and relative standard uncertainty for the heat capacities $u_r(C_{p,m}) = 0.02$ in the temperature range from $T = (6 \text{ to } 15) \text{ K}$, $u_r(C_{p,m}) = 0.005$ between $T = (15 \text{ to } 40) \text{ K}$, and $u_r(C_{p,m}) = 0.002$ in the temperature range from $T = (40 \text{ to } 344) \text{ K}$.

where \mathbf{D} is the symbol of Debye's function and n and $\Theta_{\mathbf{D}}$ are specially selected parameters. Using this equation, we obtained $n = 6$ for both tripeptides, $\Theta_{\mathbf{D}} = 56.7 \text{ K}$ for *N*-f-MLF-OH and $\Theta_{\mathbf{D}} = 62.2 \text{ K}$ for *N*-f-MLF-OMe. Using the above parameters, eq 4 describes the $C_{p,m}$ values of the compounds over the range from $T = (6 \text{ to } 12) \text{ K}$ with relative standard uncertainty $u_r(C_{p,m}) = 0.013$. In subsequent calculations, we assumed that eq 4 described the heat capacity in the range from $T = (0 \text{ to } 6) \text{ K}$ with the same relative standard uncertainty.

Standard Thermodynamic Functions. The calculations of $H(T) - H(0)$ and $S(T)$ were made by numerical integration of the curves of heat capacities with respect to T and $\ln T$,

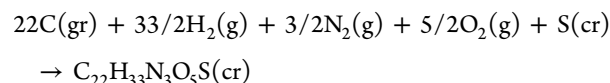
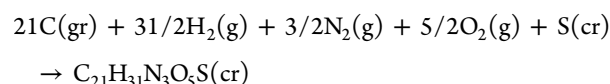
respectively (Tables 4 and 5). Gibbs energy $G(T) - H(0)$ was calculated from enthalpy and entropy values. The residual entropies of *N*-f-MLF-OH and *N*-f-MLF-OMe were assumed to be zero. The calculation procedure was described in detail elsewhere.¹⁶

Using the values of absolute entropies of tripeptides *N*-f-MLF-OH and *N*-f-MLF-OMe and that of elemental substances, including carbon,¹⁷ hydrogen,¹⁸ nitrogen,¹⁷ oxygen,¹⁸ and sulfur,¹⁸ the standard entropies of formation were calculated:

$$\Delta_f S(298.15, \text{N-f-MLF-OH, cr}) = (-2348 \pm 21) \text{ J}\cdot\text{K}^{-1}\cdot\text{mol}^{-1}$$

$$\Delta_f S(298.15, \text{N-f-MLF-OMe, cr}) = (-2448 \pm 22) \text{ J}\cdot\text{K}^{-1}\cdot\text{mol}^{-1}$$

The obtained values fit the equations:



where cr, gr, and g are crystal, graphite, and gas, respectively.

CONCLUSIONS

This work reports heat capacities of crystalline tripeptides *N*-formyl-L-Met-L-Leu-L-Phe-OH and *N*-formyl-L-Met-L-Leu-L-Phe-OMe measured over the range from $T = (6 \text{ to } 350) \text{ K}$ by precise adiabatic vacuum calorimetry. The standard thermodynamic functions of *N*-f-MLF-OH and *N*-f-MLF-OMe over the range from $T = (0 \text{ to } 350) \text{ K}$ and the standard entropies of formation at $T = 298.15 \text{ K}$ were calculated.

The low-temperature ($T \leq 50 \text{ K}$) dependencies of heat capacities were analyzed using the Debye's and the multifractal theories, and a chain-layered structures topology was established.

AUTHOR INFORMATION

Corresponding Author

*Fax: +7 831 434 50 56. E-mail: markin@calorimetry-center.ru.

Funding

This research was supported by the National Institute of Biomedical Imaging and Bioengineering of the National Institutes of Health through grants EB-003151, EB-001960, and EB-002026, and by the Ministry of Education and Science of the Russian Federation (Contract No. 14.B37.21.0799). The content is solely the responsibility of the authors and does not necessarily represent the official views of the National Institutes of Health.

Notes

The authors declare no competing financial interest.

REFERENCES

- (1) Boldyreva, E. V. Crystalline amino acids – a link between chemistry, materials sciences and biology. In *Models, mysteries, and magic of molecules*; Springer Verlag: Berlin, 2007.
- (2) Takegoshi, K.; Nakamura, S.; Terao, T. ^{13}C - ^1H dipolar-driven ^{13}C - ^{13}C recoupling without ^{13}C rf irradiation in nuclear magnetic resonance of rotating solids. *J. Chem. Phys.* **2003**, *118*, 2325–2341.

(3) Barnes, A. B.; Andreas, L. B.; Huber, M.; Ramachandran, R.; van der Wel, P. C. A.; Veshtort, M.; Griffin, R. G.; Mehta, M. A. High-resolution solid-state NMR structure of Alanine-Prolyl-Glycine. *J. Magn. Reson.* **2009**, *200*, 95–100.

(4) Lewandowski, J. R.; De Paepe, G.; Eddy, M. T.; Griffin, R. G. ^{15}N – ^{15}N proton assisted recoupling in magic angle spinning NMR. *J. Am. Chem. Soc.* **2009**, *131*, 5769–5776.

(5) Jaroniec, C. P.; Filip, C.; Griffin, R. G. 3D TEDOR NMR experiments for the simultaneous measurement of multiple carbon-nitrogen distances in uniformly ^{13}C , ^{15}N -labeled solids. *J. Am. Chem. Soc.* **2002**, *124*, 10728–10742.

(6) Bajaj, V. S.; van der Wel, P. C. A.; Griffin, R. G. Observation of a low-temperature, dynamically driven structural transition in a polypeptide by solid-state NMR spectroscopy. *J. Am. Chem. Soc.* **2009**, *131*, 118–128.

(7) Rienstra, C. M.; Tucker-Kellogg, L.; Jaroniec, C. P.; Hohwy, M.; Reif, B.; McMahon, M. T.; Tidor, B.; Lozano-Perez, T.; Griffin, R. G. De novo determination of peptide structure with solid-state magic-angle spinning NMR spectroscopy. *Proc. Natl. Acad. Sci. U.S.A.* **2002**, *99*, 10260–10265.

(8) Gavuzzo, E.; Mazza, F.; Pochetti, G.; Scatturin, A. Crystal structure, conformation, and potential energy calculations of the chemotactic peptide *N*-formyl-L-Met-L-Leu-L-Phe-OMe. *Int. J. Pept. Protein Res.* **1989**, *34*, 409–415.

(9) Varushchenko, R. M.; Druzhinina, A. I.; Sorkin, E. L. Low-temperature heat capacity of 1-bromoperfluorooctane. *J. Chem. Thermodyn.* **1997**, *29*, 623–637.

(10) Malyshev, V. M.; Mil'ner, G. A.; Sorkin, E. L.; Shibakin, V. F. Automatic low-temperature calorimeter. *Instrum. Exp. Technol.* **1985**, *6*, 195–197.

(11) Archer, D. G. Thermodynamic properties of synthetic sapphire ($\alpha\text{-Al}_2\text{O}_3$), standard reference material 720 and the effect of temperature-scale differences on thermodynamic properties. *J. Phys. Chem. Ref. Data* **1993**, *22*, 1441–1453.

(12) Della Gatta, G.; Richardson, M. J.; Sarge, S. M.; Stolen, S. Standards, calibration, and guidelines in microcalorimetry. Part 2. Calibration standards for differential scanning calorimetry. *Pure Appl. Chem.* **2006**, *78*, 1455–1476.

(13) Wieser, M. E.; Coplen, T. B. Atomic weights of the elements 2009 (IUPAC Technical Report). *Pure Appl. Chem.* **2011**, *83*, 359–396.

(14) Rabinovich, I. B.; Nistratov, V. P.; Telnoy, V. I.; Sheiman, M. S. *Thermochemical and thermodynamic properties of organometallic compounds*; Begell House: New York, 1999.

(15) Lazarev, V. B.; Izotov, A. D.; Gavrichev, K. S.; Shebershneva, O. V. Fractal model of heat capacity for substances with diamond-like structures. *Thermochim. Acta* **1995**, *269/270*, 109–116.

(16) McCullough, J. P.; Scott, D. W. *Calorimetry of Non-reacting Systems*; Butterworth: London, 1968.

(17) Chase, M. W. J. NIST-JANAF Thermochemical Tables. *J. Phys. Chem. Ref. Data* **1998**, *9*, 1–1951.

(18) Cox, J. D.; Wagman, D. D.; Medvedev, V. A. *CODATA Key Values for Thermodynamics*; Hemisphere: New York, 1989.